Implementation of Van Vleck Correction for the MWA

Pyxie Star

July 28, 2021

Quantization occurs in multiple stages of the MWA digital signal pathway and introduces small-scale nonlinearity into the data. This nonlinearity interacts with spectral structure, particularly the periodic response of the 2-stage polyphase filter banks, to result in non-negligible calibration errors. In order to achieve the sensitivity necessary for an EOR detection, the instrument spectral structure calibration must be accurate to an order of 10^{-5}. Due to the interactions between the small-scale quantization effects and the PFB structure, residual periodic response is left in the data after calibration and contaminates the power spectra. In order to cleanly remove the instrument response through calibration, we must first address the nonlinear artifacts from quantization.

Data products from the MWA are complex visibilities, that is, cross-correlations between each antenna and auto-correlations of each antenna with itself. The nonlinearity of quantization effects requires that each visibility receive a unique correction. With 8256 antenna combinations from MWA II, 768 frequencies, and 4 polarizations, this results in 10^9 computations for each 2 minute observation taken at 0.5 seconds. Thus implementations of a correction for these nonlinearities must take computational efficiency into consideration.

Formulae for correcting these artifacts with a Van Vleck correction were presented in [4]. An implementation of the correction has been written into `pyuvdata` as an option when reading raw MWA correlator output files. This memo describes MWA quantization, re-derives the correction formulae, and discusses the implementation.

1 MWA Quantization

Quantization occurs in multiple stages of the MWA digital signal pathway, with the ultimate stage being a 4 + 4 bit quantization immediately before correlation. It is this final quantization that the current implementation of the Van Vleck correction addresses. A second implementation of the Van Vleck correction is in development to address a previous quantization stage in the correlator polyphase filter bank (PFB). These quantization stages are described below in a summary of the digital signal pathway.

The analog signal from a tile is attenuated to ± 1 Volt, and a bandpass is applied to limit the frequency range to 80-300 MHz. This signal then goes to a digital receiver, described in [1], where it is sampled at 655.36 MHz and quantized to 8-bit values. The quantized data is then cast from real to complex, and also channelized into 256 1.28 MHz channels by the 'coarse' PFB. The coarse PFB has an 8 tap subfilter followed by a 512 point FFT, and functions as follows. A Kaiser windowing function is applied to 4096 data samples. The 4096 windowed samples are split into 8 'phases' of 512 samples each, which are summed to result in 512 inputs to the FFT. The FFT outputs 256 complex values each consisting of a 16-bit real and 16-bit imaginary pair. Since each frequency channel is complex, that is, carrying two sampled values, the sampling rate is halved to 327.68 MHz. The incoming data is then shifted by 512 samples and the PFB procedure applied to this next grouping. After the FFT, a gain is applied to the data, and another quantization occurs, taking the 16-bit real, 16-bit imaginary pair to a 5-bit real, 5-bit imaginary pair. For each observing session, some subset of 24 coarse channels is chosen and sent to the correlator.

The MWA correlator [2] has two stages: a 'fine' PFB which further channelizes the data, and a cross-multiply and accumulate module to perform the correlations. The fine PFB has a 12-tap subfilter that applies a Hanning window to the data stream, followed by a 128-point FFT. Outputs of the fine PFB are quantized to 4-bit real, 4-bit imaginary pairs, and these integers are cast to floats for input into the correlator cross-multiply. As discussed in [3], an asymmetric $8 + 8$ bit re-quantization occurs in the fine PFB between the subfilter and the FFT. This asymmetric rounding will be addressed by the second stage of the Van Vleck correction.

2 4-bit Van Vleck Correction

The final 4-bit quantization in the correlator is assumed to have a dominant contribution to nonlinear artifacts, and so is addressed in the initial Van Vleck implementation. For the correction model, we treat the values going into the 4-bit quantization as being sampled from an analog signal. The correction can be understood as mapping the estimated standard deviation of the distribution of a quantized signal to the estimated standard deviation of the initial analog signal. To apply the correction using visibilities, we relate the autocorrelations V_{ii} and the crosscorrelations V_{ij} to the statistical distributions of the signal. Our signals are complex, and as shown in the following sections, we are interested in the underlying statistical distribution of the real and imaginary parts of these signals. In §2.1 we lay out the relationship between an analog autocorrelation V_{11} and the standard deviation of the analog signal σ_{t_1}. Then in §2.2, the quantization pattern is used to relate an autocorrelation of quantized values $\hat{V}_{11}$ to σ_{t_1}, and thus to V_{11}. This relation provides the correction for autocorrelations. A similar analysis is performed in §2.3, relating the real and imaginary parts of an analog crosscorrelation V_{12} to the covariance between the real or imaginary parts of two signals $E[X_1X_2]$ and $E[X_1Y_2]$. The Van Vleck correction maps $E[X_1X_2]$ and $E[X_1Y_2]$ to the corresponding

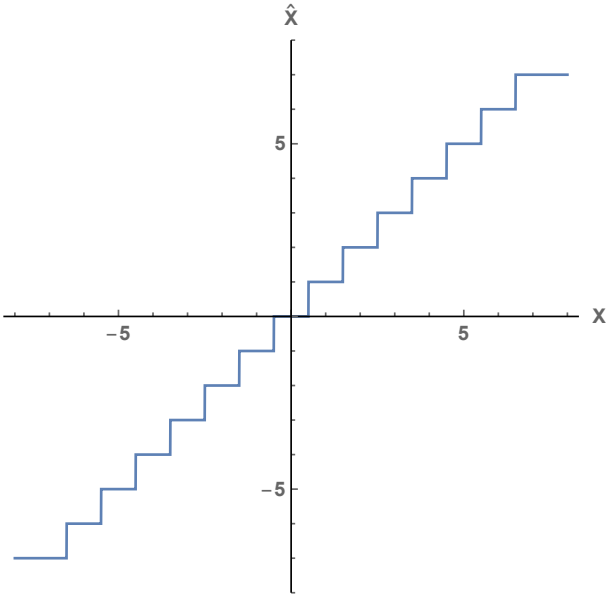

Figure 1: The 4-bit quantization pattern of the MWA.

quantized $E[\hat{X}_1\hat{X}_2]$ and $E[\hat{X}_1\hat{Y}_2]$ and thus to $\hat{V}_{12}$, as is shown in §2.4.

2.1 Analog autocorrelations

In the case of an analog signal which is sampled without quantization, let the correlator input from antenna 1 (with arbitrary polarization) be Z_1, where Z_1 is the sum of a sky signal and receiver noise: $Z_1 = S_1 + N_1$. Both S_1 and N_1 are complex circular Gaussian random variables. That is, the real and imaginary parts are each Gaussian distributed with zero mean, and are uncorrelated with each other. Alternatively, we can think of this as there being no preferred phase in either the sky signal or in the receiver noise. We additionally assume that Z_1 itself is a complex circular Gaussian random variable, which might require assumptions about the lack of correlation between sky signal and instrument noise (see Appendix A). The real and imaginary parts of Z_1 are drawn from a distribution with standard deviation σ_{t_1}. As shown below, the autocorrelation V_{11} gives an estimate of σ_{t_1}. We can write Z_1 in terms of its real and imaginary components as

$$Z_1 = X_1 + iY_1, \tag{1}$$

where X_1 and Y_1 are zero-mean Gaussian distributed. The autocorrelation is calculated by summing N samples of $Z_1 Z_1^*$. That is,

$$V_{11} = \sum_{j=1}^{N} Z_{1_j} Z_{1_j}^* \tag{2}$$

$$= \sum_{j=1}^{N} (X_{1_j} + iY_{1_j})(X_{1_j} - iY_{1_j}) \tag{3}$$

$$= \sum_{j=1}^{N} X_{1_j}^2 + \sum_{j=1}^{N} Y_{1_j}^2. \tag{4}$$

In the limit of large N, the sums can be used to approximate the second moments of X_1 and Y_1 with

$$\frac{1}{N} \sum_{j=1}^{N} X_{1_j}^2 \to E[X_1^2], \tag{5}$$

$$\frac{1}{N} \sum_{j=1}^{N} Y_{1_j}^2 \to E[Y_1^2]; \tag{6}$$

where, since X_1 and Y_1 are zero-mean Gaussian, $E[X_1^2] = \sigma_{x_1}^2$ and $E[Y_1^2] = \sigma_{y_1}^2$. Additionally, X_1 and Y_1 have the same distribution, so $\sigma_{x_1} = \sigma_{y_1}$. Thus, with sufficiently large N, we can write the autocorrelation V_{11} in terms of σ_{x_1}, an estimate of the true analog standard deviation σ_{t_1}:

$$\frac{V_{11}}{N} = \frac{1}{N} \sum_{j=1}^{N} X_{1_j}^2 + \frac{1}{N} \sum_{j=1}^{N} Y_{1_j}^2 \tag{7}$$

$$= \sigma_{x_1}^2 + \sigma_{y_1}^2 \tag{8}$$

$$= 2\sigma_{x_1}^2 \tag{9}$$

$$\simeq 2\sigma_{t_1}^2 \tag{10}$$

For later use in the Van Vleck correction, it is convenient to rewrite the above expression in the form

$$\sqrt{V_{11}/2N} = \sigma_{x_1}. \tag{11}$$

2.2 Autocorrelation correction

The 4-bit quantization sorts the real and imaginary parts of the analog signal measured by antenna 1, X_1 and Y_1, into integer bins ranging inclusively from -7 to 7, as shown in

figure 1. The autocorrelation $\hat{V}_{11}$ of these quantized samples is calculated as

$$\hat{V}_{11} = \sum_{j=1}^{N} \hat{Z}_{1_j} \hat{Z}^*_{1_j} \tag{12}$$

$$= \sum_{j=1}^{N} \hat{X}^2_{1_j} + \sum_{j=1}^{N} \hat{Y}^2_{1_j}. \tag{13}$$

Again, we use the large N limit to write

$$\frac{\hat{V}_{11}}{N} \to E[\hat{X}_1^2] + E[\hat{Y}_1^2] \tag{14}$$

$$= 2E[\hat{X}_1^2], \tag{15}$$

where, in the last line, we have used the fact that $\hat{X}_1$ and $\hat{Y}_1$ have the same distribution, thus $E[\hat{X}_1^2] = E[\hat{Y}_1^2]$. Writing in a convenient form gives

$$\hat{V}_{11}/2N \simeq E[\hat{X}_1^2]. \tag{16}$$

As outlined in [4], we use the quantization pattern to relate $E[\hat{X}_1^2]$ to σ_{x_1}, and thus $\hat{V}_{11}$ to V_{11}, as follows. The expectation value $E[\hat{X}_1^2]$ is defined

$$\begin{aligned} E[\hat{X}_1^2] =& 0^2 \cdot P(\hat{X}_1 = 0) + (-1)^2 \cdot P(\hat{X}_1 = -1) + 1^2 \cdot P(\hat{X}_1 = 1) + \cdots \\ &+ (-7)^2 \cdot P(\hat{X}_1 = -7) + 7^2 \cdot P(\hat{X}_1 = 7). \end{aligned} \tag{17}$$

The probability of $\hat{X}_1$ taking a particular quantized value is equal to the probability of X_1 falling into the corresponding quantization bin. Thus the expectation value can be written

$$\begin{aligned} E[\hat{X}_1^2] =& 0^2 \cdot P(-0.5 < X_1 < 0.5) + (-1)^2 \cdot P(-1.5 < X_1 < -0.5) + 1^2 \cdot P(0.5 < X_1 < 1.5) + \cdots \\ &+ (-7)^2 \cdot P(X_1 < -6.5) + 7^2 \cdot P(X_1 > 6.5). \end{aligned} \tag{18}$$

Taking advantage of the symmetries of both the distribution of X_1 and the quantization bins,

$$\begin{aligned} E[\hat{X}_1^2] =& 0^2 \cdot P(-0.5 < X_1 < 0.5) + 1^2 \cdot [P(-1.5 < X_1 < 1.5) - P(-0.5 < X_1 < 0.5)] + \cdots \\ &+ 7^2 \cdot [1 - P(-6.5 < X_1 < 6.5)]. \end{aligned} \tag{19}$$

With X_1 drawn from a zero-mean Gaussian distribution with σ_{t_1}, the probability that $X_1 \in [-a, a]$,

$$P(X_1 \in [-a, a]) = \operatorname{erf}\left(\frac{a}{\sigma_{t_1}\sqrt{2}}\right). \tag{20}$$

Substituting this probability and combining terms gives the compact expression

$$\begin{aligned}
E[\hat{X}_1^2] =& 0^2 \cdot \mathrm{erf}\left(\frac{0.5}{\sigma_{t_1}\sqrt{2}}\right) + 1^2 \cdot \left[\mathrm{erf}\left(\frac{1.5}{\sigma_{t_1}\sqrt{2}}\right) - \mathrm{erf}\left(\frac{0.5}{\sigma_{t_1}\sqrt{2}}\right)\right] + \cdots + 7^2 \cdot \left[1 - \mathrm{erf}\left(\frac{6.5}{\sigma_{t_1}\sqrt{2}}\right)\right] \\
=& (-1)\mathrm{erf}\left(\frac{0.5}{\sigma_{t_1}\sqrt{2}}\right) + (-3)\mathrm{erf}\left(\frac{1.5}{\sigma_{t_1}\sqrt{2}}\right) + \cdots + (-13)\mathrm{erf}\left(\frac{6.5}{\sigma_{t_1}\sqrt{2}}\right) + 7^2 \\
=& 7^2 - \sum_{k=0}^{6}(2k+1)\mathrm{erf}\left(\frac{k+0.5}{\sigma_{t_1}\sqrt{2}}\right) \\
\simeq& 7^2 - \sum_{k=0}^{6}(2k+1)\mathrm{erf}\left(\frac{k+0.5}{\sigma_{x_1}\sqrt{2}}\right). \qquad (21)
\end{aligned}$$

Using equations (11) and (16), and taking the square root of both sides, the above relation can be written in terms of V_{11} and $\hat{V}_{11}$ as

$$\boxed{\sqrt{\hat{V}_{11}/2N} \simeq \left[7^2 - \sum_{k=0}^{6}(2k+1)\mathrm{erf}\left(\frac{k+0.5}{\sqrt{V_{11}/2N}\sqrt{2}}\right)\right]^{1/2}}. \qquad (22)$$

Thus by inverting the above equation, we can obtain an estimate of the autocorrelation of analog values V_{11} from the corresponding autocorrelation of quantized values $\hat{V}_{11}$. Through calculating V_{11} we obtain σ_{x_1}, and thus can estimate the standard deviation σ_{t_1} of the analog values, which will be useful in the correction for crosscorrelations.

2.3 Analog crosscorrelations

A similar analysis can be done for the analog crosscorrelation between antenna 1 and antenna 2, V_{12}, which is calculated by summing N samples of $Z_1 Z_2^*$ so that

$$\begin{aligned}
V_{12} &= \sum_{j=1}^{N} Z_{1_j} Z_{2_j}^* && (23) \\
&= \sum_{j=1}^{N} (X_{1_j} + iY_{1_j})(X_{2_j} - iY_{2_j}) && (24) \\
&= \sum_{j=1}^{N} (X_{1_j}X_{2_j} + Y_{1_j}Y_{2_j} + iY_{1_j}X_{2_j} - iX_{1_j}Y_{2_j}). && (25)
\end{aligned}$$

The limit of large N can again be taken to give, for any combination of X_1, Y_1 with X_2, Y_2:

$$\frac{1}{N}\sum_{j=1}^{N} X_{1_j}X_{2_j} \to E[X_1 X_2]. \qquad (26)$$

Thus in this limit, the crosscorrelation

$$\frac{V_{12}}{N} \to E[X_1X_2] + E[Y_1Y_2] + iE[Y_1X_2] - iE[X_1Y_2] \tag{27}$$

$$= 2E[X_1X_2] + 2iE[Y_1X_2], \tag{28}$$

where the last step has used the following relations for circular complex random variables:

$$E[X_1X_2] = E[Y_1Y_2] \tag{29}$$

$$E[Y_1X_2] = -E[X_1Y_2] \tag{30}$$

Rewriting in terms of the real and imaginary parts of V_{12} gives

$$\begin{aligned} \mathrm{Re}\, V_{12}/2N &\simeq E[X_1X_2], \\ \mathrm{Im}\, V_{12}/2N &\simeq E[Y_1X_2]. \end{aligned} \tag{31}$$

The values $E[X_1X_2]$ and $E[Y_1X_2]$ can be related to the quantized counterparts $E[\hat{X}_1\hat{X}_2]$ and $E[\hat{Y}_1\hat{X}_2]$, as shown in the following section.

2.4 Crosscorrelation correction

We can write down the counterpart of equation (31) for the crosscorrelation of quantized values:

$$\begin{aligned} \mathrm{Re}\, \hat{V}_{12}/2N &\simeq E[\hat{X}_1\hat{X}_2], \\ \mathrm{Im}\, \hat{V}_{12}/2N &\simeq E[\hat{Y}_1\hat{X}_2]. \end{aligned} \tag{32}$$

To relate $\hat{V}_{12}$ to V_{12} we again follow [4] and use Prices's theorem, which states, for two random variables X and Y,

$$\frac{\partial\langle f(X,Y)\rangle}{\partial\langle XY\rangle} = \Big\langle \frac{\partial f}{\partial X}\frac{\partial f}{\partial Y} \Big\rangle. \tag{33}$$

where brackets indicate expectation values. Using the function $f(X_1, X_2) = \hat{X}_1\hat{X}_2$, we obtain

$$\frac{\partial E[\hat{X}_1\hat{X}_2]}{\partial E[X_1X_2]} = \Big\langle \frac{\partial \hat{X}_1}{\partial X_1}\frac{\partial \hat{X}_2}{\partial X_2} \Big\rangle. \tag{34}$$

For our quantization scheme, the derivative is composed of delta functions

$$\frac{\partial \hat{X}}{\partial X} = \delta(X - (-6.5)) + \delta(X - (-5.5)) + \cdots + \delta(X - 5.5) + \delta(X - 6.5), \tag{35}$$

which gives

$$\frac{\partial \hat{X}_1}{\partial X_1}\frac{\partial \hat{X}_2}{\partial X_2} = \sum_{i=-7}^{6}\sum_{j=-7}^{6} \delta(X_1 - (i+0.5))\delta(X_2 - (j+0.5)). \tag{36}$$

To find the expectation value, we integrate with the joint normal probability density function

$$\Big\langle \frac{\partial \hat{X}_1}{\partial X_1}\frac{\partial \hat{X}_2}{\partial X_2}\Big\rangle = \sum_{i=-7}^{6}\sum_{j=-7}^{6}\int_{-\infty}^{\infty}\int_{-\infty}^{\infty} dX_1 dX_2 \delta(X_1-(i+0.5))\delta(X_2-(j+0.5)) \\ \frac{1}{2\pi\sigma_1\sigma_2\sqrt{1-\rho^2}}\exp\Big[-\frac{1}{2(1-\rho^2)}\Big(\frac{X_1^2}{\sigma_{t_1}^2}+\frac{X_2^2}{\sigma_{t_2}^2}-\frac{2\rho X_1 X_2}{\sigma_{t_1}\sigma_{t_2}}\Big)\Big], \tag{37}$$

where $\rho = E[X_1X_2]/\sigma_{t_1}\sigma_{t_2}$. This gives

$$\Big\langle \frac{\partial \hat{X}_1}{\partial X_1}\frac{\partial \hat{X}_2}{\partial X_2}\Big\rangle = \sum_{i=-7}^{6}\sum_{j=-7}^{6}\frac{1}{2\pi\sigma_{t_1}\sigma_{t_2}\sqrt{1-\rho^2}}\exp\Big[-\frac{1}{2(1-\rho^2)}\Big(\frac{(i+0.5)^2}{\sigma_{t_1}^2}+\frac{(j+0.5)^2}{\sigma_{t_2}^2} \\ -\frac{2\rho(i+0.5)(j+0.5)}{\sigma_{t_1}\sigma_{t_2}}\Big)\Big] \tag{38}$$

Writing $E[X_1X_2] = \rho\sigma_{t_1}\sigma_{t_2}$, equation 34 becomes

$$\frac{\partial E[\hat{X}_1\hat{X}_2]}{\partial\rho} = \sum_{i=-7}^{6}\sum_{j=-7}^{6}\frac{1}{2\pi\sqrt{1-\rho^2}}\exp\Big[-\frac{1}{2(1-\rho^2)}\Big(\frac{(i+0.5)^2}{\sigma_{t_1}^2}+\frac{(j+0.5)^2}{\sigma_{t_2}^2} \\ -\frac{2\rho(i+0.5)(j+0.5)}{\sigma_{t_1}\sigma_{t_2}}\Big)\Big]. \tag{39}$$

With equation (32) and $\sigma_{x_1} \simeq \sigma_{t_1}$,

$$\frac{\operatorname{Re}\hat{V}_{12}/2N}{\partial\rho} \simeq \sum_{i=-7}^{6}\sum_{j=-7}^{6}\frac{1}{2\pi\sqrt{1-\rho^2}}\exp\Big[-\frac{1}{2(1-\rho^2)}\Big(\frac{(i+0.5)^2}{\sigma_{x_1}^2}+\frac{(j+0.5)^2}{\sigma_{x_2}^2} \\ -\frac{2\rho(i+0.5)(j+0.5)}{\sigma_{x_1}\sigma_{x_2}}\Big)\Big]. \tag{40}$$

An integration over both sides gives the Van Vleck correction for the crosscorrelations:

$$\boxed{\operatorname{Re}\hat{V}_{12}/2N \simeq \sum_{i=-7}^{6}\sum_{j=-7}^{6}\int_0^{\rho} d\rho'\frac{1}{2\pi\sqrt{1-\rho'^2}}\exp\Big[-\frac{1}{2(1-\rho'^2)}\Big(\frac{(i+0.5)^2}{\sigma_{x_1}^2}+\frac{(j+0.5)^2}{\sigma_{x_2}^2} \\ -\frac{2\rho'(i+0.5)(j+0.5)}{\sigma_{x_1}\sigma_{x_2}}\Big)\Big].} \tag{41}$$

With equation (31), $\rho \simeq \operatorname{Re}V_{12}/2N\sigma_{x_1}\sigma_{x_2}$, and so the above function corrects the real part of the crosscorrelation. The imaginary part is corrected by simply substituting $\operatorname{Im}V_{12}$ and $\operatorname{Im}\hat{V}_{12}$ for $\operatorname{Re}V_{12}$ and $\operatorname{Re}\hat{V}_{12}$, respectively.

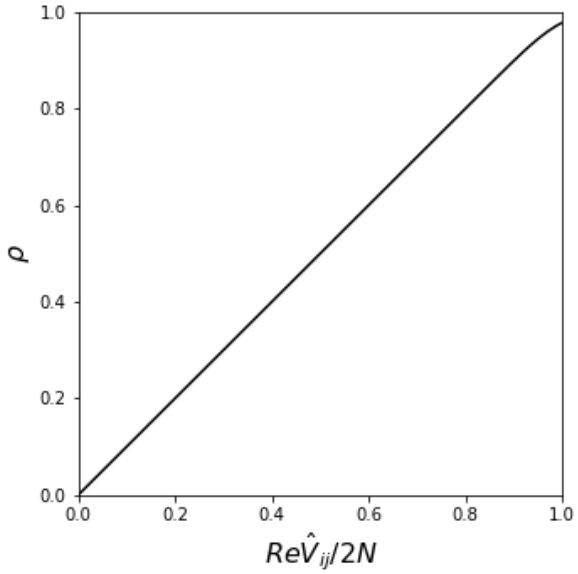

Figure 2: The cross-correlation Van Vleck correction function (equation 41) plotted with $\sigma_{x_1} = 1.0, \sigma_{x_2} = 1.0$.

3 Implementation

To apply the Van Vleck correction, the data is first scaled by $1/2N$. A square root is then taken of the autocorrelations to obtain $\sqrt{\hat{V}_{ii}/2N}$. Equation (22) is used to estimate $\sqrt{V_{ii}/2N}$ and thus also σ_{x_i}. The values for σ_{x_i} and σ_{x_j} are then used in equation (41) to obtain estimates of the real and imaginary parts of $V_{ij}/2N$ from $\hat{V}_{ij}/2N$.

The Van Vleck correction algorithm is implemented in `pyuvdata`. To verify the algorithm, equations (22) and (41) were plotted, as shown in figures 2 and 3. Comparison plots were then generated using the implementations of these functions in the code, verifying the functions' accuracy. Also, data corrected by the algorithm was taken back through equations (22) and (41), showing that the calculated quantized data matched the initial uncorreted input.

Equation (22) is not invertible, so Newton's method for finding roots is used to iteratively solve the equation

$$0 = \sqrt{\hat{V}_{11}/2N} - \left[7^2 - \sum_{k=0}^{6}(2k+1)\mathrm{erf}\left(\frac{k+0.5}{\sqrt{V_{11}/2N}\sqrt{2}}\right)\right]^{1/2}. \tag{42}$$

A similar method was implemented for equation (41). However, the correction algorithm has a high computational cost due to the 14^2 exponential terms, which were each eval-

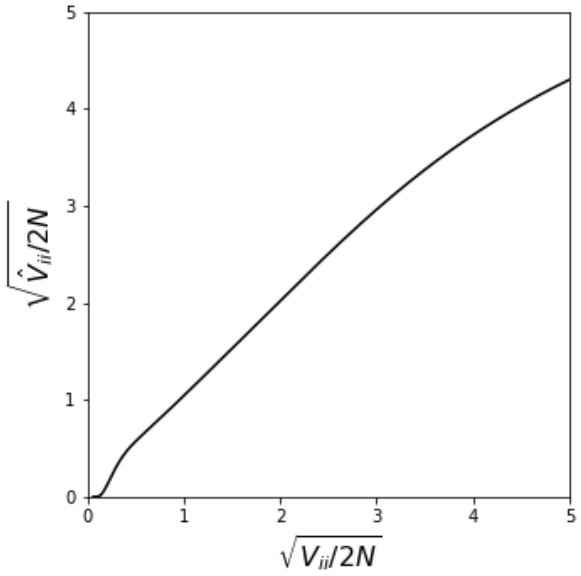

Figure 3: The auto-correlation Van Vleck correction function (equation 22).

uated ~ 10 times to compute the integral. By combining redundant terms, this number was reduced by a factor of 2. Though only ~ 5 evaluations of equation (41) were required for the root-finding function to converge, the computation time remained prohibitively long at ~ 5 hours per observation. To address this, an approximation using Chebychev polynomials was implemented which brings the correction time to $\sim$ 30 minutes per observation.

Equation (41) was fit to the following function

$$\rho = c1 \cdot T_1(\kappa) + c3 \cdot T_3(\kappa) + c5 \cdot T_5(\kappa), \tag{43}$$

where T_k is the kth Chebyshev polynomial and κ is either the real or imaginary part of $\hat{V}_{ij}/2N$. A two-dimensional grid of (σ_{x_i}, σ_{x_j}) was created, with values ranging between 0.9-4.5 and grid spacing 0.01. For each pair (σ_{x_i}, σ_{x_j}), a fitting function solved for the coefficients $c1, c3, c5$. These coefficients were saved and are imported into the Van Vleck correction function. For each crosscorrelation in the data, a bisection search finds the indices for the nearest σ_{x_i} and σ_{x_j} in the grid. A bilinear interpolation algorithm uses these indices to obtain the coefficients $c1$, $c3$, and $c5$. These coefficients are used in equation (43) to correct both the real and imaginary parts of $\hat{V}_{ij}/2N$.

A single MWA observation taken at 0.5 second time resolution and 40 kHz frequency resolution has $\sim 10^{10}$ crosscorrelations. To apply a unique correction to each of these values in a time scale on the order of the time to read the files, the bilinear interpola-

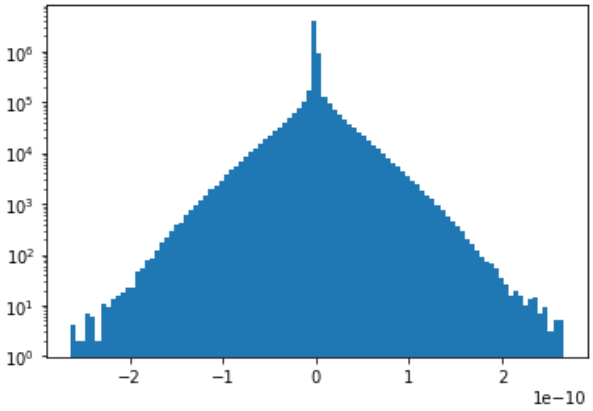

Figure 4: Differences between scaled crosscorrelations corrected using both an iterative integral solver and the Chebyshev approximation. These differences are on order 10^{-10}, which is the scale at which the integral solver tests solutions. This suggests that using the Chebyshev approximation does not decrease the accuracy of solutions.

tion and Chebyshev evaluation stages were implemented in cython. This modification brought the correction time to ~ 30 minutes in addition to the ~ 12 minute read time.

To check the Chebyshev polynomial approximation, a single timestamp of 2013 crosscorrelations was corrected both with an iterative integral solver and with the Chebyshev implementation. The differences between the resulting values are of order 10^{-10}, as seen in figure 4. As the iterative solver finds solutions that are accurate to 10^{-10}, these differences indicate no change in accuracy in results obtained with the Chebyshev approximation.

A Circular Complex Gaussian Random Variables

A circular complex random variable $Z = \mathrm{Re}(Z) + i\,\mathrm{Im}(Z)$ is defined as having a distribution that is invariant under a random phase shift:

$$E[Z] = E[e^{i\phi}Z] = 0, \tag{44}$$

$$E[ZZ] = E[e^{i\phi}Ze^{i\phi}Z], \tag{45}$$

$$E[ZZ^*] = E[e^{i\phi}Ze^{-i\phi}Z^*]]. \tag{46}$$

The last of these conditions is trivial. The first and second are only satisfied if $E[Z] = E[ZZ] = 0$. Thus

$$E[ZZ] = 0 \tag{47}$$

$$= E[(\mathrm{Re}(Z) + i\,\mathrm{Im}(Z))(\mathrm{Re}(Z) + i\,\mathrm{Im}(Z))] \tag{48}$$

$$= E[\mathrm{Re}(Z)^2] - E[\mathrm{Im}(Z)^2] + iE[\mathrm{Re}(Z)\,\mathrm{Im}(Z)] + iE[\mathrm{Im}(Z)\,\mathrm{Re}(Z)] \tag{49}$$

and

$$E[\mathrm{Re}(Z)^2] = E[\mathrm{Im}(Z)^2], \tag{50}$$
$$E[\mathrm{Re}(Z)\,\mathrm{Im}(Z)] = -E[\mathrm{Im}(Z)\,\mathrm{Re}(Z)] = 0. \tag{51}$$

For a complex random variable, the variance $\sigma_Z^2 = E[ZZ^*] = E[\mathrm{Re}(Z)^2] + E[\mathrm{Im}(Z)^2]$. So in the case of a circularly complex random variable

$$\sigma_Z^2 = 2E[\mathrm{Re}(Z)^2] = 2E[\mathrm{Im}(Z)^2]. \tag{52}$$

Two circular complex random variables sampled from the same distribution have the following relations

$$E[\mathrm{Re}(Z_1)\,\mathrm{Re}(Z_2)] = E[\mathrm{Im}(Z_1)\,\mathrm{Im}(Z_2)] \tag{53}$$
$$E[\mathrm{Re}(Z_1)\,\mathrm{Im}(Z_2)] = -E[\mathrm{Im}(Z_1)\,\mathrm{Re}(Z_2)] \tag{54}$$

If this relation does not hold for circular complex random variables sampled from different distributions, then some assumptions are required for the correlator input model.

For example, consider the case of a correlator input $Z = S + N$, where S and N are both circular complex Gaussian random variables, that is, in addition to the conditions above, the real and imaginary parts of S and N are sampled from zero-mean Gaussian distributions. To treat Z as circularly complex requires $E[\mathrm{Re}(Z)\,\mathrm{Im}(Z)] = 0$. Thus

$$E[\mathrm{Re}(S)\,\mathrm{Im}(S)] + E[\mathrm{Re}(N)\,\mathrm{Im}(N)] + E[\mathrm{Re}(S)\,\mathrm{Im}(N)] + E[\mathrm{Re}(N)\,\mathrm{Im}(S)] = 0. \tag{55}$$

The first two terms vanish according to (51). If (54) applies to circular complex random variables sampled from different distributions, the last two terms vanish. If the relation does not apply, then it is required that $E[\mathrm{Re}(S)\,\mathrm{Im}(N)] = E[\mathrm{Re}(N)\,\mathrm{Im}(S)] = 0$, that is, that the sky signal and receiver noise are uncorrelated.

References

[1]T. Prabu et al., "A digital-receiver for the murchison widefield array", Experimental Astronomy **39(1)**, 73–93 (2015).

[2]S. M. Ord et al., "The murchison widefield array correlator", Publications of the Astronomical Society of Australia **32** (2015).

[3]S. J. McSweeney et al., *Mwa tied-array processing iii: microsecond time resolution via a polyphase synthesis filter*, 2020 PREPRINT.

[4]L. V. Benkevitch et al., *Van vleck correction generalization for complex correlators with multilevel quantization*, 2015.

[5]A. M. Levine, *An analysis of two cascaded fourier transforms and application to the coarse and fine pfbs for the mwa*, 2012.

[6] A. M. Levine, *The effects of the two-stage pfb architecture on the response of the mwa*, 2012.

[7] A. Beardsley, "The murchison widefield array 21cm epoch of reionization experiment: design, construction, and first season results", PhD thesis (University of Washington, Seattle, WA, 2015).